

## Comparative analysis of pollutants emission by classical and distributed propulsions applied on the AOS motor glider

Comparative analysis of harmful compounds emission of classical and distributed propulsions applied on the AOS motor glider, taking into account the perspective of the development of hybrid propulsions. A novel path is indicated by so-called distributed aircraft propulsion. The advantages and disadvantages of this type of solutions are presented, as well as the conceptual design of the distributed propulsion for the AOS 71 motor glider. In the paper there were compared the emissions of harmful compounds generated by a hybrid power unit developed for the airframe of AOS 71 motor glider – traditional propulsion, so-called focused (one-propeller) and dispersed propulsion (multi-propelled). Functional diagrams of both types of propulsions solutions are presented. Construction and aerodynamic constraints of both propulsions are discussed and comparative analysis is made. In the traditional version of the propulsion (so-called focused propulsion), the propeller is driven by an Emrax 228 electric engine with effective parameters:  $N = 55 \text{ kW}$ ,  $M = 120 \text{ Nm}$ . The power source is a battery set with a capacity of 16 Ah and a range extender powered by a LCR 407ti rotating piston engine with maximum power of 28 kW. In the variant of the distributed propulsion. Ten electric engines of AXI 8120 type were used to drive small propellers arranged along the wingspan. The power source in this variant is analogous to the variant with the Emrax electric engine. For the adopted variant of the flight mission of the motor glider, a flight trajectory model was developed, which was used to determine the load of the power unit. In laboratory conditions, emission tests of both propulsions were conducted. The results are summarized in charts and discussed in the conclusions.

Key words: distributed propulsion, hybrid, motor glider, rotary engine, Wankel engine, hybrid propulsion, emission, exhaust gases

### Introduction

The electric and hybrid propulsion is becoming a more and more interesting alternative to conventional propulsion systems used in aircraft. In the case of new types of constructions there appear the problems with increased mass of the power unit or limited range due to low battery capacity [1, 19]. To improve the parameters of electric or hybrid propulsion, research on distributed propulsion is being conducted [1, 19]. Figure 1 presents the concept of an experimental LeapTech aircraft (a consortium of LeapTech and NASA) equipped with an electric distributed propulsion. According to calculations made by the aircraft's designers, the lift coefficient increased by 3 times due to the appropriate aerodynamic design of the propulsion – acceleration of the stream over the wing.

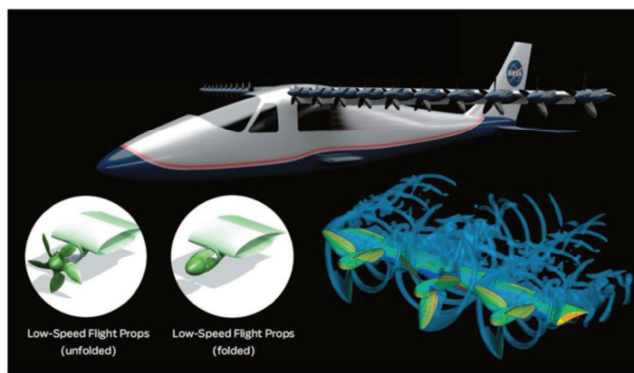


Fig. 1. The LeapTech aircraft [1]

Figure 2 shows the type of the UAV (Unmanned Aerial Vehicle) of the NASA construction, enabling vertical start.



Fig. 2. The UAV of NASA construction [19]

The distributed propulsion is based on the use of a series of low power engines placed along the wingspan or in the appropriate places of the hull. The total thrust generated by such a power unit is sufficient for the safe operation of the aircraft. In addition, the method of integrating the engines with the airframe can affect the aerodynamic performance of the aircraft. It is also possible to reduce or eliminate control surfaces by properly differentiating (vectoring) the engines thrust. The conducted research brings interesting results (improvement of aerodynamic parameters – increase of the lift coefficient, etc. [1, 14]).

The paper describes a comparative analysis in terms of both pollutant emissions and performance for the hybrid power unit of the AOS-71 motor glider of classical and distributed propulsion.

### 1. Research object

As the basis for the analysis the airframe of the AOS-71 electric glider (Fig. 3) was assumed. The aircraft was built in cooperation between the Department of Aircraft and Aircraft Engines at the Rzeszow University of Technology

and the Faculty of Power and Aeronautical Engineering at the Warsaw University of Technology.



Fig. 3. The AOS 71 motor glider

In Table 1 the basic data of the airframe are presented, and in Fig. 4 the values of power required for the flight in relation to the flight speed.

Table 1. Basic data of the AOS 71 motor glider) [11, 12]

Wing area	S [m <sup>2</sup> ]	15.8
Wing span	R [m]	16.4
Aspect ratio	$\Delta$	17
Maximum take-off mass	M <sub>max</sub> [kg]	660
Minimum motor glider mass	M <sub>min</sub> [kg]	500

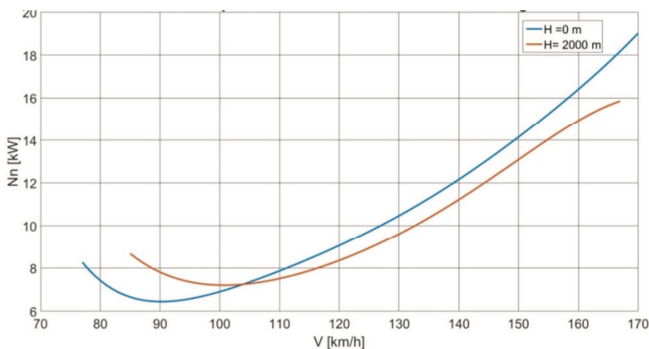


Fig. 4. Power required for flight in the function of flight speed – for the AOS 71 motor glider; M<sub>max</sub> = 660 kg [11, 12]

The power source for the analysed propulsions is a hybrid system in which a small battery set cooperates with an electric generator driven by a rotary piston (Wankel AG 407TG<sub>i</sub>). Table 2 shows the technical data of the engine and battery assembly.

Table 2. Technical data of power unit [11, 12, 16]

Engine		407TG <sub>i</sub>
Maximum engine power	N <sub>max</sub> [kW]	31.5
Maximum torque	M <sub>max</sub> [Nm]	51
Engine mass	m <sub>s</sub> [kg]	20
Specific fuel consumption	SFC <sub>min</sub> [kg/kWh]	0.3
Battery	–	Li-Pol
Capacity	C [Ah]	16
Voltage	U <sub>bat</sub> [V]	355
Battery mass	m <sub>bat</sub> [kg]	50

For the internal combustion engine, the rotational characteristics was determined in order to adjust properly the range of its work to the generator's work (Emrax 188). In addition, the emission of pollutants in the exhausts of the 407TG<sub>i</sub> engine was determined in the function of its rotational speed with used Horiba analyzer. Measurements were made on the research stand in the Department of Aircraft and Aircraft Engines. Figures 5–9 show the test stand, the rotational characteristics of the internal combustion engine and the NO<sub>x</sub>, CO and CO<sub>2</sub> emissions.



Fig. 5. The engine characteristics testing stand

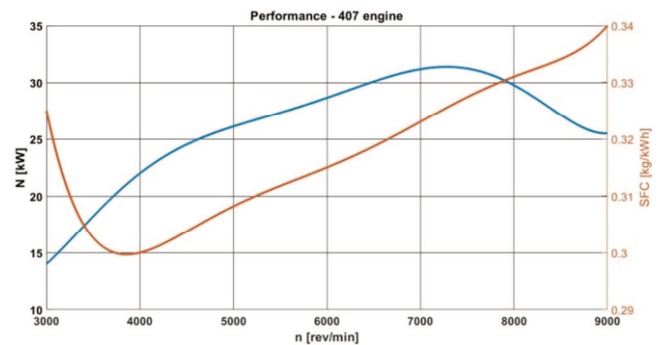


Fig. 6. Rotational characteristics of the 407 engine

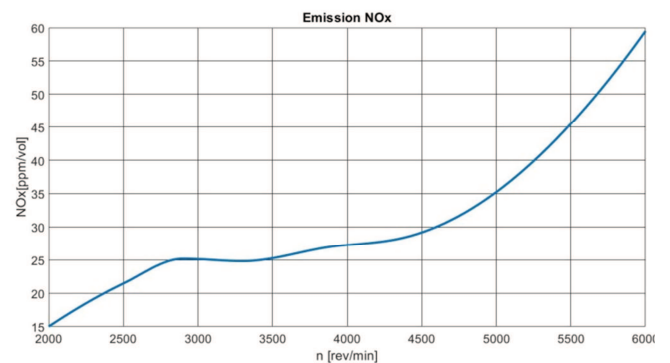


Fig. 7. The NO<sub>x</sub> emission of the 407TG<sub>i</sub> engine

The analysis of the charts presented in the Figs 7–9, leads to the following conclusions:

1. The CO<sub>2</sub> and CO emissions were the lowest in the vicinity of the maximum torque obtained by the engines (about 4000 rpm), which at the same time was a point close to minimum of specific fuel consumption.

2. The NO<sub>x</sub> emission grew continuously in the function of rotational speed, which was associated with the increase in the combustion temperature and the increase in fuel consumption by the engines [10, 13].

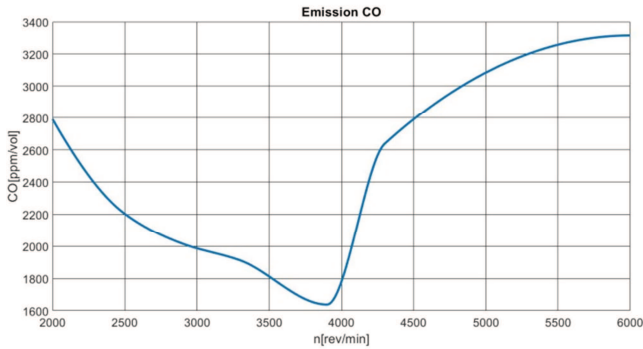


Fig. 8. The CO emission of the 407TGi engine

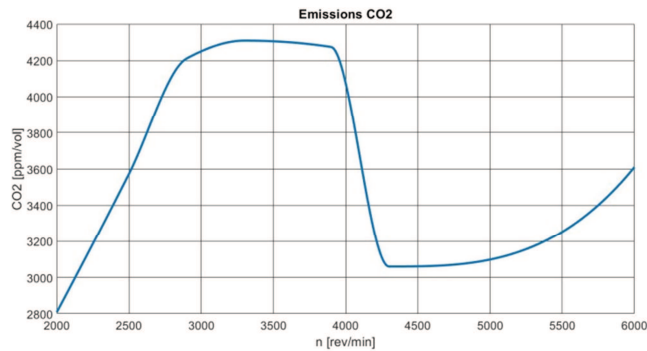


Fig. 9. The CO<sub>2</sub> emission of the 407TGi engine

The results obtained were used to conduct further research and analyses.

## 2. Selection of the distributed propulsion for the airframe

Taking into account the aerodynamic parameters of the airframe and the maximum power developed by the classic power unit, ten BLDC AXI 8120/10 engines were selected for the variant of distributed propulsion. The parameters of this engine are shown in Table 3.

Table 2. Technical data of AXI 8120/10[17]

Engine Type	BLDC	–
Maximum engine power	N <sub>max</sub> [kW]	4.2
No load current	I <sub>0</sub> [A]	1.2
Maximum current	I <sub>IN</sub> [A]	95
Maximum voltage	U <sub>IN</sub> [V]	44.5
Engine pulse	K <sub>v</sub> [RPM/V]	140
Voltage	R <sub>M</sub> [Ω]	0.00466

Figure 10 presents a visualization of the distribution of engines installed on the motor glider.

Based on the technical data of the AXI 8120/10 [17] engine, its rotational characteristics were determined for the selection of propellers (Fig. 11). For this purpose, the formulas (1),(2),(3) were used to determine the input and output power (received on the shaft) of the engine. In this case the motor voltage control is assumed.

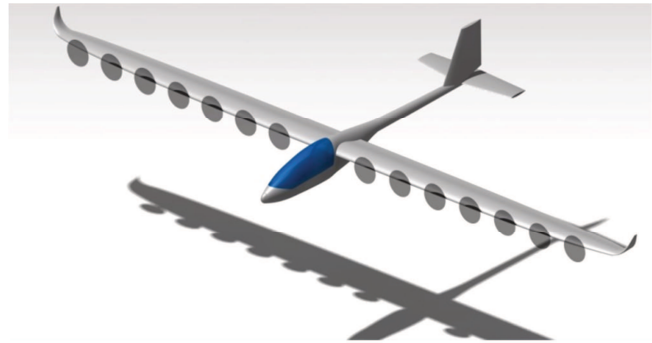


Fig. 10. Visualization of the propulsion concept

$$N_{IN} = I_{IN} \cdot U_{IN} \tag{1}$$

where N<sub>IN</sub> – engine input power [W], I<sub>IN</sub> – input current [A], U<sub>IN</sub> – input voltage[V].

$$N_{OUT} = (I_{IN} - I_0) \cdot (U_{IN} - I_{IN} \cdot R_M) \tag{2}$$

where N<sub>OUT</sub> – engine output power[W].

$$n = K_v \cdot (U_{IN} - I_{IN} \cdot R_M) \tag{3}$$

where n – engine revolution [rev/min].

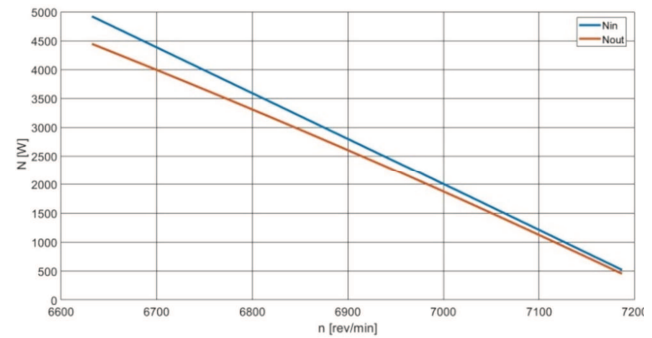


Fig. 11. The rotational characteristics of the AXI 8120/10 engine

Based on the calculated performance of the electric engine, using the available characteristics of the propeller [4, 8, 14] a two-blade propeller with a Clark Y2 profile and a diameter of 220 mm was selected. Such propellers allowed to determine the thrust of the power unit [4, 8] as the function of the flight speed of the motor glider. This is shown in Fig. 12.

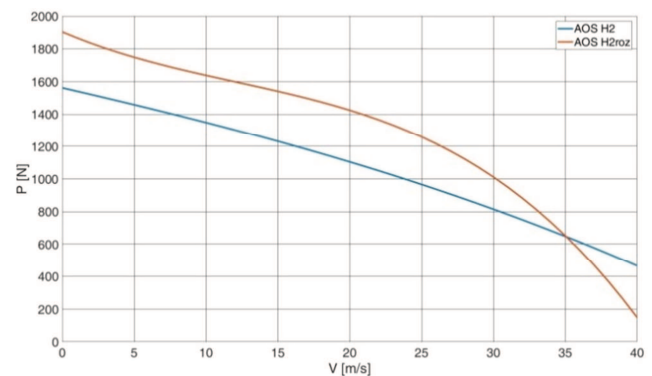


Fig. 12. Comparison of the thrust generated by distributed (red) and classical (blue) propulsions

This graph was used to determine the performance of the motor glider for both power units and for their comparison.

### 3. Comparison of the obtained power units performances and pollutants emission

For the assumed mission profile (i.e. start and flight, set at the altitude of 600 m, as illustrated in Fig. 13), the emission of individual compounds generated on a given route in the control volume was determined, assuming:

- The range until the energy source is depleted,
- The ambient conditions corresponding to the parameters according to the International Standard Atmosphere at a given altitude and the lack of wind.

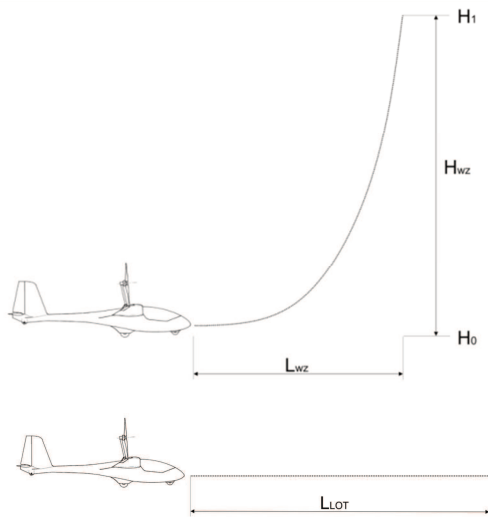


Fig. 13. Flight profile – climb (up) and horizontal flight (down)

On the basis of the chart presented in Fig. 12 and the aerodynamic data, it can be concluded that the classical propulsion, taking into account the efficiency of the propeller, consumes about 9 kW from the power source to generate thrust required for the flight. Under the same flight conditions, the distributed propulsion needs about 80% of this power to generate the same thrust.

Using the formula (4), the energy required for an hour of flight for both types of propulsions was determined:

$$E_h = x \cdot (N_n \cdot t_h) \div \eta_{sm} \quad (4)$$

where:  $t_h$  – flight time (1 h),  $N_n$  – power required for flight,  $x$  – number of engines (10 distributed, 1 classical).

Based on the formula (5), the energy stored on-board was determined:

$$E = I \cdot 3600[s] \cdot U_{bat} + \eta_{gen} \cdot (N_s \cdot t_s) \quad (5)$$

where:  $t_s$  – generator operation time [1]:

$$t_s = \frac{m_{fuel}}{SFC \cdot N_s} \quad (6)$$

$N_s$  – power of rotary engine, SFC – specific fuel consumption 407 Tgi engine,  $m_{fuel}$  – mass of fuel stored on-board the aircraft (7 kg).

The total flight time was determined by:

$$t_L = E/E_h \quad (7)$$

Based on the calculations, for both drives there were determined the flight time and the corresponding range for a flight speed equal to 100 km/h. The results are shown in Figs 14 and 15.

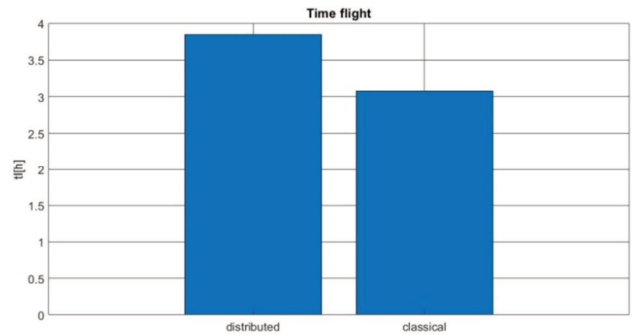


Fig. 14. The flight time

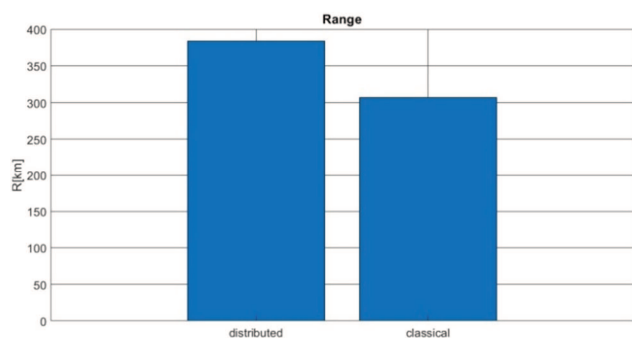


Fig. 15. The motor glider's range

The conducted research allowed to determine the emission for both propulsions. For comparative purposes, in Figs 16–18 the pollutants emissions during distance flight of 300 km are presented.

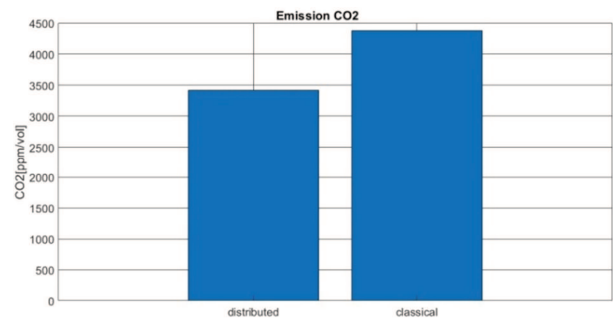


Fig. 16. The CO<sub>2</sub> emission

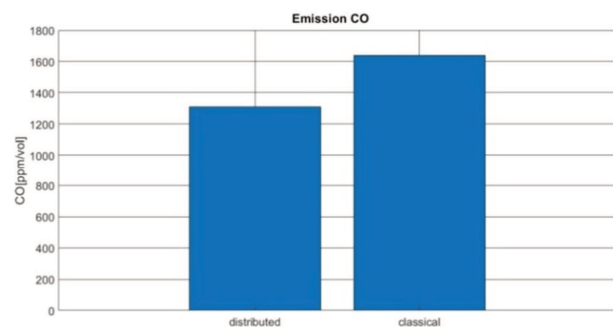


Fig. 17. The CO emission

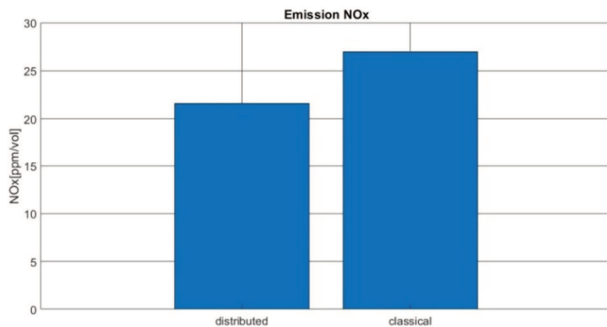


Fig. 18. The NO<sub>x</sub> emission

#### 4. Conclusion

The analysis conducted leads to the following conclusions:

1. For the distributed propulsion, the range has increased by 76 kilometers and the flight duration by 46 minutes.

#### Bibliography

- [1] ALEX, M. et al. Drag reduction through distributed electric propulsion. *Aviation Technology, Integration, and Operations Conference*. Atlanta 16-20 June 2014.
- [2] ANDERSON, J. Introduction to flight. *McGraw Hill Book Company*. San Francisco 2003.
- [3] BOJOI, R., BOGGERO, H., et al. Multiphase drives for hybrid-electric propulsion in light aircrafts: a viable solution. *Conference: 2018 International Symposium on Power Electronics, Electrical Drives, Automation and Motion (SPEEDAM)*. DOI: 10.1109/SPEEDAM.2018.8445241
- [4] BUKOWSKI, J., ŁUCJANEK, W. Napęd śmigłowy teoria i konstrukcja. *MON*. Warszawa 1984.
- [5] GEISS, I., VOIT-NITSCHMANN, R. Sizing of fuel-based energy systems for electric aircrafts. *Proceedings of the Institution of Mechanical Engineers Part G-Journal of Aerospace Engineering*. 2017, **231**. DOI: 10.1177/0954410017721254
- [6] FAHIM, M. An overview of double-bar single-wheel rotary combustion engine. *Advances in Mechanical Engineering*. 2019, **11**(2), 1-13. DOI: 10.1177/1687814019828074
- [7] HENDERSON, R.P., MARTINS, J.R.R.A., PEREZ, R.E. Aircraft conceptual design for optimal environmental performance. *The Aeronautical Journal*. 2012, **116**(1175), 1-22.
- [8] HARTMAN, E., BIEDERMAN, D. The aerodynamic characteristic of full-scale propellers. *NACA Report No. 640*, 1938.
- [9] JAKUBOWSKI, R., ORKISZ, M. A review of selected alternative propulsion systems for UAV applications. *Zeszyty Naukowe/Wyższa Szkoła Oficerska Sił Powietrznych Dęblin*. 2015, **231**.
- [10] KOTLARZ, W. Turbinowe zespoły napędowe źródłem skażeń powietrza na lotniskach wojskowych. *Wyższa Szkoła Oficerska Sił Powietrznych*. Dęblin 2003.
- [11] MARIANOWSKI, J., FRĄCZEK, W., CZARNOCKI, F. Założenia podstawowe dla projektu motoszybowca AOS-H2. (*not publish*)
- [12] MARIANOWSKI, J., TOMASIEWICZ, J., CZARNOCKI, F. Analiza masowa motoszybowca AOS-H2. (*not publish*)
- [13] PAWLAK, M. Metoda modelowania emisji szkodliwych i toksycznych składników spalin turbinowych silników odrzutowych samolotów pasażerskich w warunkach przelotowych. *Wyd. Uniwersytetu Morskiego w Gdyni*. Gdynia 2019.
- [14] ROSKAM, J. *Airplane Aerodynamics and Performance*, DARcorporation. Kansas 2016.
- [15] SINGH, V. Perceptions of emission reduction potential in air transport: a structural equation modeling approach. *Environment Systems and Decisions*. 2016, **36**(4), 377-403.
- [16] WANKEL AG, Wankel engine manual
- [17] [www.axi-motors.com](http://www.axi-motors.com)
- [18] [www.emrax.com](http://www.emrax.com)
- [19] [www.nasa.gov](http://www.nasa.gov)

Prof. Marek Orkisz, DSc., DEng. – Faculty of Mechanical Engineering and Aeronautics, Rzeszow University of Technology.  
e-mail: [mareko@prz.edu.pl](mailto:mareko@prz.edu.pl)



Piotr Wygonik, DEng. – Faculty of Mechanical Engineering and Aeronautics, Rzeszow University of Technology.  
e-mail: [piowyg@prz.edu.pl](mailto:piowyg@prz.edu.pl)



Michał Kuźniar, MEng. – Faculty of Mechanical Engineering and Aeronautics, Rzeszow University of Technology.  
e-mail: [mkuzniar@prz.edu.pl](mailto:mkuzniar@prz.edu.pl)



Maciej Kalwara, MEng. – Faculty of Mechanical Engineering and Aeronautics, Rzeszow University of Technology.  
e-mail: [kalmac@prz.edu.pl](mailto:kalmac@prz.edu.pl)

